

Turbulence effects on supernova neutrinos

James Kneller*

*Institut de Physique Nucléaire, F-91406 Orsay cedex,
CNRS/IN2P3 and University of Paris-XI, France and
Department of Physics, North Carolina State University, Raleigh, NC 27695, USA*

Cristina Volpe†

*Institut de Physique Nucléaire, F-91406 Orsay cedex,
CNRS/IN2P3 and University of Paris-XI, France*

Multi-dimensional core-collapse supernova simulations exhibit turbulence of large amplitude and over large scales. As neutrinos pass through the supernova mantle the turbulence is expected to modify their evolution compared to the case where the explosion is free of turbulence. In this paper we study this turbulence effect upon the neutrinos modelling the turbulence expected from multi-dimensional simulations by adding matter density fluctuations to density profiles taken from one-dimensional hydrodynamical simulations. We investigate the impact upon the supernova neutrino transition probabilities as a function of the neutrino mixing angle θ_{13} and turbulence amplitude. In the high (H) resonant channel and with large θ_{13} values we find that turbulence is effectively two flavor for fluctuation amplitudes $\lesssim 1\%$ and have identified a new effect due to the combination of turbulence and multiple H resonances that leads to a sensitivity to fluctuations amplitudes as small as $\sim 0.001\%$. At small values of θ_{13} , beyond the range achievable in Earth based experiments, we find that turbulence leads to new flavor transient effects in the channel where the MSW H resonance occurs. Finally, we investigate large amplitude fluctuations which lead to three flavor effects due to broken HL factorization and significant non-resonant transitions and identify two non-resonant turbulence effects, one depending on the θ_{13} , and the other independent of this angle and due to the low (L) MSW resonance.

PACS numbers: 97.60.Bw,14.60.Pq,11.30.Er

Keywords:

I. INTRODUCTION

Core-collapse supernova simulations have reached a high degree of sophistication and complexity in the last decade. A new picture is emerging that shows how several ingredients might be necessary to achieve successful explosions. These include fluid instabilities (the SASI mode), realistic nuclear networks, detailed neutrino transport, rotation, magnetic fields etc. [1, 2]. The flavor evolution of the neutrino signal from the next Galactic supernova as a function of time and energy has the potential to reveal invaluable information about the explosion of the star and is being thoroughly investigated for the case of spherically symmetric explosions.

Fully understanding neutrino flavor conversion in the supernova environment and the complex interplay with the various features of the supernova dynamics is clearly a theoretical challenge. Nevertheless, there has been significant ongoing progress and recent developments have highlighted a variety of novel flavor conversion phenomena. This is due to the inclusion of both the neutrino-neutrino interaction and the use of dynamic density pro-

files taken from simulations. While the former induces collective effects [3–8] the latter produces dynamic multiple Mikheev-Smirnov-Wolfenstein (MSW) resonances which can lead to phase effects [9–16]. For a review see [17, 18]. The first calculation for the supernova neutrino signal implementing both of these effects together consistently is performed in [19] while the impact of collective and dynamic MSW effects upon the diffuse supernova neutrino background can be found in [20, 21].

Multi-dimensional supernova simulations indicate strong turbulence, particularly in the region between the reverse and forward shocks, generated by non-radial fluid flow through the distorted shock surfaces [22–24] and other multi-dimensional phenomena. But due to the absence of suitable multi-dimensional simulations important properties of the turbulence, such as its amplitude at late times, are unknown. Turbulence effects upon neutrinos, not just in supernova, have been investigated in several works [25–28]. In [29] neutrino oscillations in noisy media with δ -correlated fluctuations is considered with applications to a fluctuating matter density and magnetic fields in the sun. In [29] it is also found that depolarization can also occur even if the fluctuations never cause the density to cross the neutrino resonance density i.e. they are off-resonance. The application to supernovae is studied in [30] with a similar model for the turbulence to determine the implications for neutrino flavor conversion

*Electronic address: jim.kneller@ncsu.edu

†Electronic address: volpe@ipno.in2p3.fr

and supernova dynamics (r-process and shock reheating). In [31] the authors use the same model of delta-correlated fluctuations for core-collapse supernovae, but now with profiles containing both front and reverse shocks. A sensitivity to the third neutrino mixing angle is shown in the channels where no MSW H resonance occurs (electron neutrino channel in inverted hierarchy and electron anti-neutrino channel in normal hierarchy). Finally arguments were made in [32] about the application of Kolmogorov correlated fluctuations and linear profiles to supernova. Regardless of their differences, all these studies agree that the inclusion of matter density fluctuations in media has the possible consequence of producing completely mixed states (a process called ‘depolarization’) if the amplitude is sufficiently large. At the same time all these investigations are based on the solutions of differential equations for the averaged density matrix using just two neutrino flavors. The first full three flavor study of turbulence effects is performed in Ref.[33] where turbulence is superimposed upon profiles from one-dimensional hydrodynamical simulations using a Kolmogorov spectrum for the density fluctuations. In contrast to the previous work, here turbulence effects are studied by building a statistical ensemble of instantiations for the neutrino survival probability. It is also shown there that HL factorization might be broken in the limit of strong turbulence. But despite the acknowledgment that turbulence may be important the effect is not considered in the calculations for the neutrino signal. Thus it remains unclear if the presence of turbulence will remove the information about the explosion imprinted in the neutrino signal and which is supposed to indicate the missing information about neutrino mixing.

The purpose of this paper is to revisit the subject of turbulence effects upon core-collapse supernova and explore the effects of changing the angle θ_{13} and the turbulence amplitude. As in Ref. [33] we follow the neutrino evolution in the star using matter density profiles from a one-dimensional hydrodynamical simulation with Kolmogorov correlated turbulence superimposed. Similarly we construct an ensemble of results computed using a phase-retaining 3-flavor integrator instead of determining the average density matrix and survival probabilities. We then investigate the distributions of the probabilities and compute the mean and the variance in order to study how the effects we find evolve as a function of the parameters. Our paper is structured as follows: in Section II the model and the numerical procedures are described, Section III presents the numerical results of turbulence effects on the survival probabilities first for the case of small amplitude turbulence and both large and small θ_{13} and then large amplitude fluctuations which can cause three flavor mixing in both the H-resonant and non-H-resonant channel, Section IV contains our conclusions.

II. THE MODEL

Neutrinos evolve through matter according to the Schroedinger-like equation:

$$i \frac{d}{dt} |\psi\rangle = H |\psi\rangle = (K + V) |\psi\rangle. \quad (1)$$

In the absence of neutrino-neutrino interactions the Hamiltonian is composed of two terms: the vacuum term K , and the potential term V due to the matter. In the flavor basis the vacuum term $K^{(f)}$ depends upon two mass-square differences δm_{12}^2 and δm_{23}^2 and on the parameters of the Maki-Nakagawa-Sakata-Pontecorvo matrix which are the three neutrino mixing angles usually labeled as θ_{12} , θ_{13} , θ_{23} and three phases, one Dirac and two Majorana. For all results in this paper we set the oscillation frequencies and angles to $\delta m_{12}^2 = 8 \times 10^{-5} \text{eV}^2$, $|\delta m_{23}^2| = 3 \times 10^{-3} \text{eV}^2$ and by $\sin^2 2\theta_{12} = 0.83$ and $\sin^2 2\theta_{23} = 1$ [34]. We shall consider both normal and inverse hierarchies and various values for the unknown angle θ_{13} up to its limit from Chooz [35, 36]. We do not consider any effect coming from the Dirac CP phase δ . For a discussion of its impact see [8, 37].

The potential term, at some fixed time is diagonal in the flavor basis i.e. $V^{(f)}(\mathbf{r}) = \text{diag}(V_e(\mathbf{r}), V_\mu(\mathbf{r}), V_\tau(\mathbf{r}))$ with $V_e(\mathbf{r}) = \sqrt{2} G_F n_e(\mathbf{r})$ and $n_e(\mathbf{r})$ the electron density. The potentials $V_\mu(\mathbf{r})$ and $V_\tau(\mathbf{r})$ are negligible compared to $V_e(\mathbf{r})$ and will be ignored hereafter. The turbulence we shall study in this paper enters into equation (1) through n_e so in order to compute the neutrino evolution one needs to provide a density profile from which we can construct V_e . Ideally a study of the effect of turbulence in supernova upon the neutrinos would use density profiles taken from successful multi-dimensional core-collapse supernova simulations. While significant progress continues to be made in the sophistication of the simulations we are still far from being able to extract fluctuation characteristics (scale, power spectra and amplitude) from them at late times and in the outer regions of the supernova where our interest lies. Therefore one must adopt a pragmatic approach by using a ‘turbulence’ free explosion and then adding the turbulence to it in some prescribed fashion [31, 33]. The scale, power spectrum and amplitude of the turbulence are thus variable. While this approach requires calibration before it can be applied to understanding turbulence in multi-dimensional supernova simulations, an exploration of the turbulence parameter space can discover general features of turbulence effects upon the neutrinos. There are also several advantages of this approach: first, the underlying profile is the same so that non-turbulent features - such as the shocks - are always located at the same positions, second the turbulence in the profiles of the members of an ensemble is uncorrelated, and third, if the turbulence has a zero expectation value then the average potential $\langle V \rangle$ is known exactly allowing us to compare the effects of turbulence to the situation when turbulence is absent.

Now that we have outlined our approach we spell out

the details. We start with a profile taken from a spherically symmetric simulation, i.e. a one dimensional model. We shall ensure that this one dimensional profile is also the average profile $\langle V \rangle(r)$ once the turbulence is added. The one-dimensional density profile we employ is the 4.5 s snapshot taken from the hydrodynamical simulation of Ref.[38] with $Q = 3.36 \times 10^{51}$ erg. This particular simulation was chosen because it has the greatest resemblance with the 2D hydrodynamical simulations there and because the density of the region between the shocks - into which we will add the turbulence - overlaps with the H resonance density for neutrino energies between 10 and 80 MeV as shown in Galais *et al.* [21]. Although we show results for a given snapshot in time our findings are valid for the entire period the shock wave is in the H resonance region for neutrino energies of order $\mathcal{O}(10 \text{ MeV})$ i.e. from $t \sim 2 \text{ s}$ to $t \sim 10 \text{ s}$ or so. Later the shocks will move to affect the L resonance but the neutrino flux will be so small at these times that turbulence effects may be well-nigh impossible to observe. The turbulence is included in the model by writing the potential term in Eq.(1) as

$$V(r) = (1 + F(r)) \langle V \rangle(r) \quad (2)$$

with $F(r)$ a random field. The field $F(r)$ is constructed as

$$F(r) = \frac{C_\star}{\sqrt{N_k}} \tanh\left(\frac{r - r_r}{\lambda}\right) \tanh\left(\frac{r_s - r}{\lambda}\right) \times \sum_{n=1}^{N_k} \{A_n \cos[k_n(r - r_r)] + B_n \sin[k_n(r - r_r)]\} \quad (3)$$

for $r_r \leq r \leq r_s$ and is zero outside this range. In this equation the parameter C_\star sets the amplitude of the fluctuations. The two radii r_r and r_s are the positions of the reverse and forward shock respectively; the two tanh terms are included to suppress fluctuations close to the shocks and prevent discontinuities at r_s and r_r , and the parameter λ is a scale over which the fluctuations reach their extent size. We set $\lambda = 100 \text{ km}$. The second half of equation (3) is the discrete Fourier representation of a random field. The members of the set of co-efficients $\{A\}$ and $\{B\}$ are independent standard Gaussian random variates with zero mean thus ensuring the vanishing expectation value of F . To determine the N_k k 's, A 's and B 's for an instantiation of F the 'Randomization method' described in Ref.[39] is employed. The number of modes used throughout most of this paper is $N_k = 100$ but to assure the reader that this is sufficient we shall also compute one of our principal results using $N_k = 1000$ so that the reader can observe that the results for $N_k = 100$ are essentially similar. Finally, the wavenumber cutoff k_\star is set to $k_\star = \pi/(r_s - r_r)$ i.e. a wavelength twice the distance between the shocks. The power spectrum $E(k)$ we use is

$$E(k) = (\alpha - 1) \left(\frac{k_\star}{k}\right)^\alpha. \quad (4)$$

Throughout this work we shall adopt a Kolmogorov spectrum where $\alpha = 5/3$. Note that the power spectrum in Eq.(4) is very different from the one of the δ -correlated power spectra of Refs.[30] and [31].

Now that all terms in Eq.(1) are defined, we solve the three flavor neutrino evolution equation with the phase-retaining integrator of Ref.[40]. The quantities we are interested in calculating, are the neutrino and antineutrino survival and appearance probabilities, i.e. $P(\nu_j \rightarrow \nu_i)$ and $P(\bar{\nu}_j \rightarrow \bar{\nu}_i)$, in the matter basis since the flux of neutrinos emerging from the star is given by these quantities, multiplied by the appropriate initial fluxes at the proto-neutron star. The relationship between the flavor and matter bases can be found in Kneller & McLaughlin [40]. Such probabilities can be formed from the wavefunction for each initial pure state or from the elements of the S -matrix. For brevity we shall often use the notation $P_{ij} = P(\nu_j \rightarrow \nu_i)$ and $\bar{P}_{ij} = P(\bar{\nu}_j \rightarrow \bar{\nu}_i)$.

III. NUMERICAL RESULTS: TURBULENCE IMPACT ON THE PROBABILITIES

Our aim is to explore the parameter space of our model in order to survey the various effects turbulence produces and derive the relationships between the survival and crossing probabilities as a function of the parameters. This represents a large undertaking, for now we shall limit our parameter space to the mixing angle θ_{13} and the fluctuation amplitude C_\star and shall reserve for a later date [41] an exploration of the effects of changes in the turbulence power spectrum, the snapshot profile and the turbulence location. In particular we shall not consider the effect of turbulence in front of the forward shock, an issue intimately tied to the observability of neutrino transformation effects in the neutrino burst from the next galactic supernova.

We begin with the case of large θ_{13} and explore the effects in the H resonant channel before considering smaller values of θ_{13} . We shall finish with the effects of large amplitude fluctuations that can break HL factorization and lead to large effects in the non-resonant channels.

A. Effective two flavor mixing in the H resonant channel

By following the neutrino as it progresses through the profile for a given instantiation we discover that the effect of turbulence can span a range from the perturbative to the strong. First, turbulence introduces many new H resonances which lead to substantial changes from the evolution of the same neutrino through the profile sans turbulence. We also observe the perturbative effect caused by non-resonant fluctuations i.e. those fluctuations of the density that approach, but do not intersect, the resonance density. These two limits, the strong and the perturbative, can be seen in figure (1) where we show the

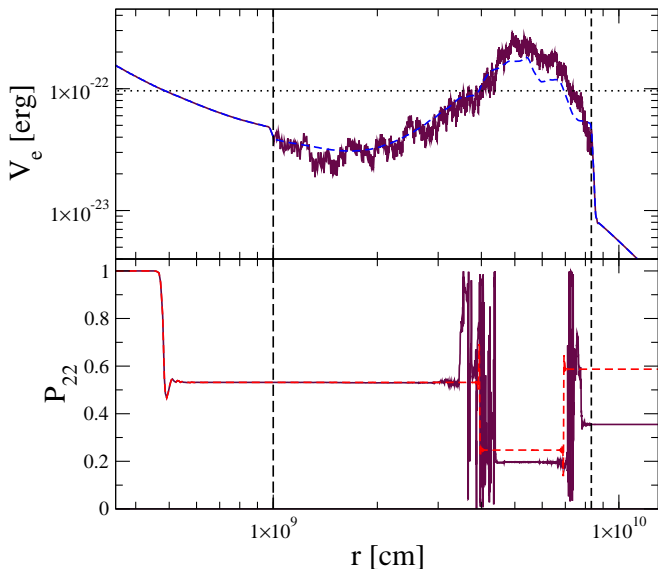


FIG. 1: One instantiation of the density profile (top panel) and the survival probability $P_{22} = P(\nu_2 \rightarrow \nu_2)$ for a $E = 25$ MeV neutrino (bottom panel) as functions of the radius r . The turbulence region is identified by the vertical dashed lines in both panels, the H resonance density is the horizontal line in the upper panel determined using the two flavor formula. The underlying base profile is shown as the dashed line in the upper panel, the evolution through the base profile as the dashed line in the lower panel. The value of θ_{13} is $\sin^2(2\theta_{13}) = 4 \times 10^{-4}$, the hierarchy is normal, and the amplitude of the density fluctuations is $C_*^2 = 0.1$.

evolution of the second matter eigenstate survival probability, P_{22} (lower panel), as a function of the radius r through one instantiation of the matter density profile (top panel). The results are for a ‘large’ value [42] of θ_{13} corresponding to $\sin^2 2\theta_{13} = 4 \times 10^{-4}$, a 25 MeV neutrino and the normal hierarchy. We see that without fluctuations the neutrino experiences just three H resonances for this chosen profile and energy, and one is located outside the turbulence region. After the inclusion of turbulence the number of MSW resonances increases significantly. Since such resonances are semi-adiabatic for this value of θ_{13} the presence of the extra resonances due to turbulence causes the neutrino survival probability to undergo large transitions as the neutrino passes through them. This can be seen more clearly in figure (2), an enlargement of figure (1). At each new H resonance caused by a downward fluctuation of the density the matter mixing angle $\tilde{\theta}_{13}$ will swing from a value close to its high density limit of 90° through 45° towards its vacuum value and then back again: for an upward fluctuation that crosses the resonance density the matter mixing angle does the opposite swinging from close to the vacuum value up towards 90° and then down again. Either way, the non-adiabaticity parameter Γ_{23} [40] - which describes the mixing between matter states ν_2 and ν_3 - is proportional to

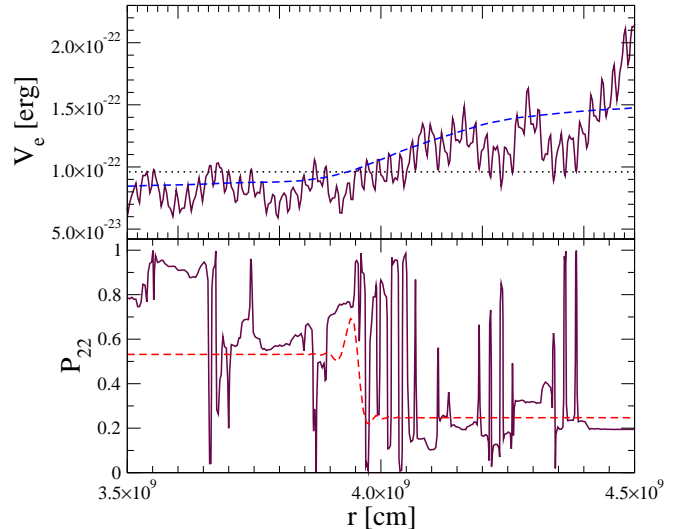


FIG. 2: An enlargement of figure (1) to show the detailed neutrino evolution in the MSW H resonance region.

the derivative $d\tilde{\theta}_{13}/dr^1$. Γ_{23} is largest in the region of the resonance and if ever $\Gamma_{23} \gtrsim 1$ then we have significant mixing between states ν_2 and ν_3 and thus a change in the survival probability P_{22} . Similar results are obtained for the antineutrino matter eigenstate survival probabilities $\bar{P}_{11} = P(\bar{\nu}_1 \rightarrow \bar{\nu}_1)$ and $\bar{P}_{33} = P(\bar{\nu}_3 \rightarrow \bar{\nu}_3)$ in the case of inverted hierarchy because now it is the antineutrino non-adiabaticity $\bar{\Gamma}_{13}$ which is proportional to the derivative $d\tilde{\theta}_{13}/dr$ and the H resonance mixes states $\bar{\nu}_1$ and $\bar{\nu}_3$.

Figure (2) also allows us to observe the perturbative effect from non-resonant fluctuations. At non-resonant fluctuations the matter mixing angle $\tilde{\theta}_{13}$ now varies over a smaller extent. The closer the fluctuation approaches the resonance the larger the variation. Despite the smaller variation of $\tilde{\theta}_{13}$ at a non-resonant fluctuation compared to a resonant fluctuation the evolution of the neutrino state is governed by the *derivative* of this angle which can be large. For this reason we understand why non-resonant fluctuations can lead to the evolution of P_{22} as observed.

The evolution of a neutrino with a particular energy and some set of oscillation parameters through the turbulent density profile is unique for each instantiation of

¹ More exactly one observes that both the Γ_{23} and the Γ_{13} non-adiabaticity parameters defined in [40] are proportional to $d\tilde{\theta}_{13}/dr$ but as a consequence of the evolution of the matter mixing angle $\tilde{\theta}_{12}$ in a normal hierarchy the non-adiabaticity function Γ_{13} is suppressed.

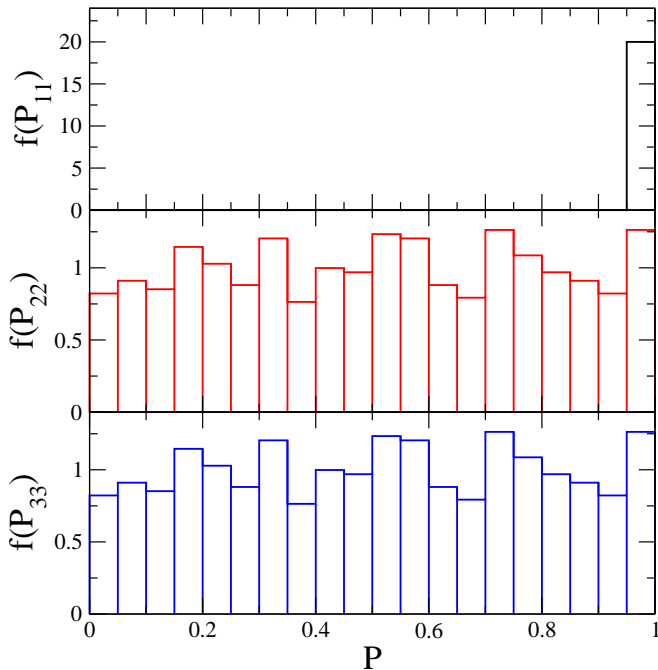


FIG. 3: A normalized frequency histogram of 1012 calculations of P_{11} (top panel) P_{22} (middle panel) and P_{33} (bottom panel) for $E = 25$ MeV neutrinos. The hierarchy is normal, $\sin^2(2\theta_{13}) = 4 \times 10^{-4}$ and $C_\star^2 = 0.01$.

the turbulence. If we change the F then we find a completely different final state. If we repeat this exercise many times then we can construct an ensemble of final states from which we can study the general net effect of the turbulence i.e. the state of the neutrino after it has passed through the entire turbulence region and exits the supernova. The results of such an exercise are shown in figure (3) which displays the survival probability distribution of the three neutrino matter eigenstates in the case of $E = 25$ MeV neutrinos, a normal hierarchy, $\sin^2(2\theta_{13}) = 4 \times 10^{-4}$ and $C_\star^2 = 0.01$. Since mixing at the H resonance is between states ν_2 and ν_3 and also the amplitude of the fluctuation is relatively small the survival probability P_{11} is a delta-function at $P_{11} = 1$. Larger fluctuation amplitudes lead to broken HL factorization [33]. In contrast one can see that the distributions for P_{22} and P_{33} are consistent with uniform and the average of the ensemble for these two probabilities is $1/2$. This implies that full ‘depolarization’ occurs for matter states ν_2 and ν_3 : one starts with a pure neutrino state and ends up with a flavor state that is completely random so that all information of the initial state is lost in the averages.

As we decrease the fluctuation amplitude the number of new resonances created tends to zero and also the perturbative effect from non-resonant fluctuations disappears. But surprisingly we find that the turbulence does not disappear quickly with C_\star . Turbulence continues to

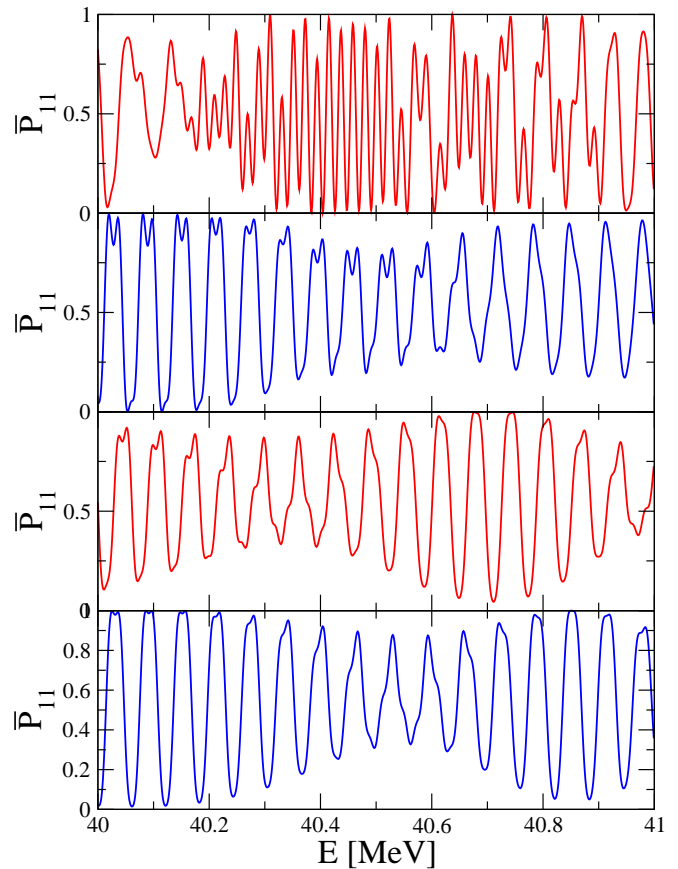


FIG. 4: A very fine energy resolution of \bar{P}_{11} between 40 and 41 MeV. The bottom panel is for no fluctuations, the next is $C_\star = 10^{-3}$, then $C_\star = 10^{-2}$ and $C_\star = 10^{-1}$. The results correspond to inverted hierarchy and a ‘large’ third neutrino mixing angle given by $\sin^2(2\theta_{13}) = 4 \times 10^{-4}$.

have a large impact upon the final state probabilities one finds in an ensemble even for fluctuation amplitudes as small as $C_\star \sim 10^{-5}$. We have investigated the reason for this extreme sensitivity and have found that it is due to a change in the relative phase difference between the extant resonances of the profile. That the sensitivity to small C_\star is due to the combination of phase effects and turbulence can be deduced from figure (4). Here the hierarchy is inverted but this makes no difference to the argument. Going from the lower to upper panels one can see that for values of $C_\star = 10^{-3} - 10^{-2}$ the turbulence does not change the correlation energy scale of ~ 50 keV. Only for $C_\star \gtrsim 10^{-1}$ does one observe a decrease in the correlation energy scale to ~ 10 keV as the turbulence effects start dominating over the phase effects. From the similarity of the middle panels of the figure with the case of no fluctuations one concludes that the number of resonances must be the same for all of them. Once this is appreciated one can then understand the sensitivity to C_\star

from the case of two resonance phase effects discussed in Kneller & McLaughlin [15] and Dasgupta & Dighe [16]. Using a two-flavor approximation of the mixing between states α and β the crossing probability for a neutrino passing through two resonances is

$$P_C = P_1(1 - P_2) + (1 - P_1)P_2 + 2\sqrt{P_1 P_2(1 - P_1)(1 - P_2)} \cos \Phi \quad (5)$$

where $P_i(r_i)$ are the crossing probabilities for the resonances separately and

$$\Phi = \int_{r_1}^{r_2} dr(k_\alpha - k_\beta) \quad (6)$$

is an interference term in which the r 's are the locations of the resonances and the k 's are the matter eigenvalues. Turbulence leads to fluctuations of $k_\alpha - k_\beta$, relative to the case without turbulence, and it also shifts the resonance positions r_1 and r_2 . But if the fluctuation amplitude is small the changes in the resonance positions and the gradient there are also small and so P_1 and P_2 are essentially unaltered. This leaves just the fluctuations of Φ due to the small shifts in the resonance positions and the difference of the eigenvalues $k_\alpha - k_\beta$ between them. In order to generate a large effect we need a change $\delta\Phi \sim 1$ but this is typically small compared to Φ itself which is often $\Phi \gg 1$ because the resonances are very far apart. If $\delta\Phi \sim 1$ then P_C will vary over the range $\Delta P_C = 4\sqrt{P_1 P_2(1 - P_1)(1 - P_2)}$ and one may show that $\Delta P_C \leq 1/2$ i.e. less than the spread of the uniform distribution shown above.

So with this understanding of how neutrinos can be sensitive to such small amplitude fluctuations we present the full evolution of the survival and crossing probabilities as a function of C_\star for this case of a normal hierarchy and 'large' θ_{13} . Figures (5) and (6) show plots of the probabilities P_{11} , P_{12} , P_{22} and P_{23} as a function of the matter density fluctuation amplitude for 60 MeV neutrinos in a normal hierarchy with $\sin^2 2\theta_{13} = 4 \times 10^{-4}$. The energy has changed compared to previous figures simply for the sake of clarity of the figure, the results are otherwise typical. And to demonstrate that the results are insensitive to the number of k modes we present results for $N_k = 100$ in figure (5) and in figure (6) $N_k = 1000$. From these figures four different ranges of C_\star can be identified. For values smaller than $C_\star^2 \lesssim 10^{-10}$ turbulence effects are negligible and the probabilities one derives are always the same and determined by the MSW resonances of the underlying adopted profile. For values between $C_\star^2 \sim 10^{-10}$ and 10^{-2} the turbulence effects and the phase effects induced by the multiple MSW resonances of the underlying profile, that must occur even in the absence of fluctuations, combine to produce broad variations over the ensemble but smaller than the depolarization limit. In the figures one observes that the rms variance of P_{22} and P_{23} plateau at $\sigma = 0.23$, whereas the two flavor depolarized limit would give $\sigma = 0.28$. In the region 10^{-2} - 10^{-1} turbulence effects start dominating over phase effects and

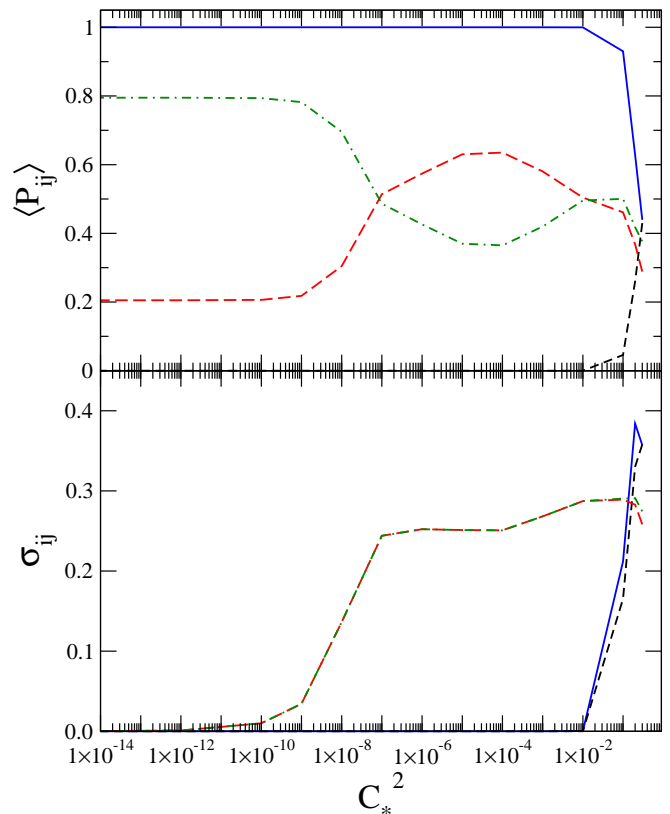


FIG. 5: The mean and the variance of the neutrino matter survival probabilities for a $E = 60$ MeV neutrino, as a function of the noise amplitude. At every value of C_\star these quantities are calculated from at least 1000 samples of the turbulence F . The mean and rms variance of P_{11} is represented by the solid line in both panels, P_{22} is shown by the long-dashed, P_{12} and P_{23} are the short-dashed and dash-dot lines respectively. The hierarchy is normal and $\sin^2(2\theta_{13}) = 4 \times 10^{-4}$. The number of k modes is $N_k = 100$.

lead to depolarization of states ν_2 and ν_3 but not ν_1 . Note that figure (3) shows the distribution for the survival probabilities when C_\star is in this range and one observes in figures (5) and (6) that σ reaches 0.28 for these values of C_\star . Finally, for $C_\star^2 \gtrsim 0.1$ we start to transit to the case of three flavor depolarization where all three matter states start to mix due to broken HL factorization [33]. The distributions start to become triangular and the mean value drops towards $1/3$. This transition to three flavor mixing is studied more carefully in the next section.

Investigating how turbulence effects are modified when one decreases θ_{13} is important because the third neutrino mixing angle may not turn out to be close to the present Chooz limit and able to be measured in the forthcoming reactor and first superbeam experiments. In a core-collapse supernova without turbulence, the non-adiabaticity of the H resonances of profiles from spherically symmetric simulations becomes large for values of θ_{13} smaller than the Dighe-Smirnov threshold of

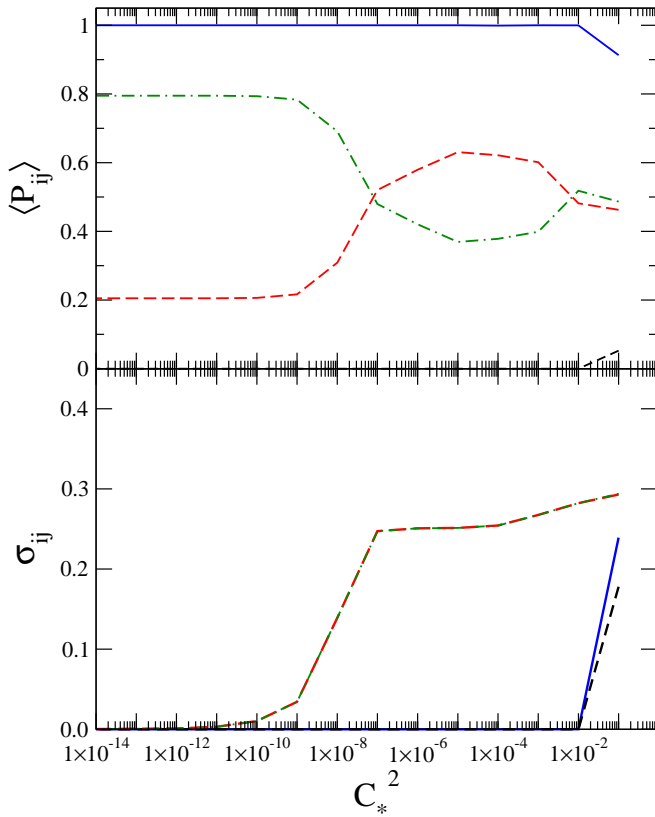


FIG. 6: The same as figure (5) but with $N_k = 1000$.

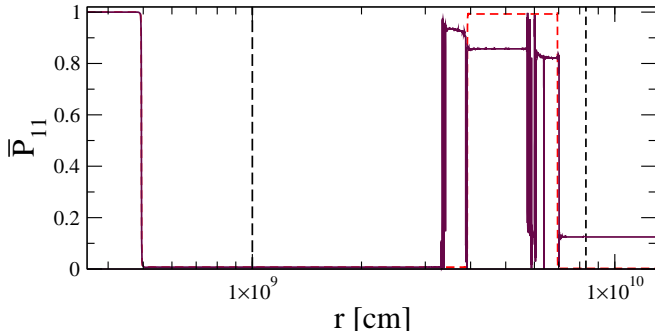


FIG. 7: The survival probability \bar{P}_{11} for a $E = 25$ MeV antineutrino as functions of the radius r but now with the value of θ_{13} set to $\sin^2(2\theta_{13}) = 4 \times 10^{-6}$. The instantiation of the density is shown in figure (1). Again, the turbulence region is identified by the vertical dashed lines and the evolution through the base profile as the dashed line. The hierarchy is inverted and the fluctuation amplitude is $C_* = 0.1$.

$\sin^2 2\theta_{13} \sim 10^{-5}$ [42]. But when we include turbulence the limiting behavior that survival probabilities for the states that mix at the H resonance should tend to zero as $\theta_{13} \rightarrow 0$ need not occur because the smallness of any non-zero θ_{13} can always be compensated by increasing the amplitude and/or extent of the matter fluctuations. However the fluctuation amplitude cannot be increased

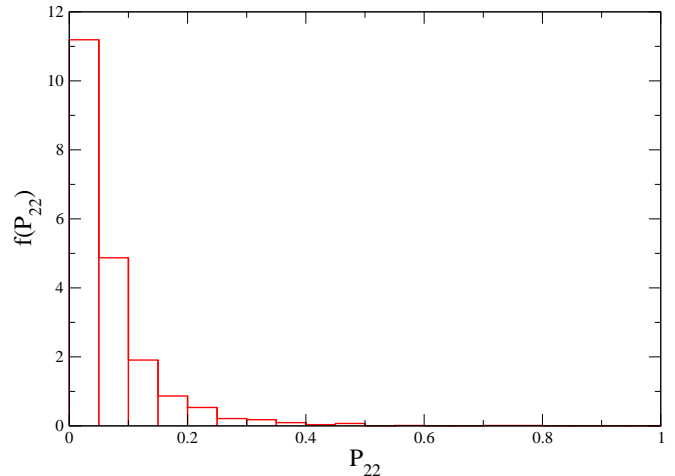


FIG. 8: A normalized frequency histogram of 1687 calculations of P_{22} for a $E = 25$ MeV neutrino with a fixed underlying profile and $C_* = 0.1$. Here θ_{13} is set to $\sin^2(2\theta_{13}) = 4 \times 10^{-6}$ and the hierarchy normal.

beyond reason and the region where turbulence occurs is limited to the space between the shocks in our model. It is due to these ‘upper limits’ on the compensating variables that indeed we can expect to reach the limiting behavior of non-adiabatic evolution for the H resonant mixing states as $\theta_{13} \rightarrow 0$ at some point but note it will not necessarily be at the same value as the Dighe-Smirnov threshold. This expectation is borne out when one investigates the effect of turbulence for small values of θ_{13} since one observes there can be significant, i.e. greater than $\mathcal{O}(1\%)$, changes in the neutrino survival probability for values of $\sin^2 2\theta_{13} = 4 \times 10^{-6}$, as shown in figure (7). For this particular figure the hierarchy is inverted so the H resonance mixes the antineutrino states $\bar{\nu}_1$ and $\bar{\nu}_3$, for a normal hierarchy mixing is between ν_2 and ν_3 but the essential behavior is the same for both.

As for the case of large θ_{13} , each instantiation of F leads to a different final state and again we can construct the distribution of the possible final states by Monte Carlo methods. The distribution of the final state P_{22} for the case of a normal hierarchy, $E = 25$ MeV, $\sin^2(2\theta_{13}) = 4 \times 10^{-6}$ and $C_* = 0.1$ is shown in figure (8). We see that the distribution is not a delta-function at zero corresponding to non-adiabatic propagation but rather appears to have an exponential behavior.

With figure (9) we summarize the entire behavior of the turbulence effect as a function of θ_{13} for a fixed matter density fluctuation amplitude $C_* = 0.1$. For ‘large’ angles - above the Dighe-Smirnov threshold- we are in the depolarized limit for this value of $C_* = 0.1$, below the threshold we are in a scaling regime where $P_{22} \propto \theta_{13}^2$. Setting a limit that observable changes require $\langle P_{22} \rangle \geq 0.01$ for present neutrino detectors then we see that turbulence induces observable sensitivity to θ_{13} for values above

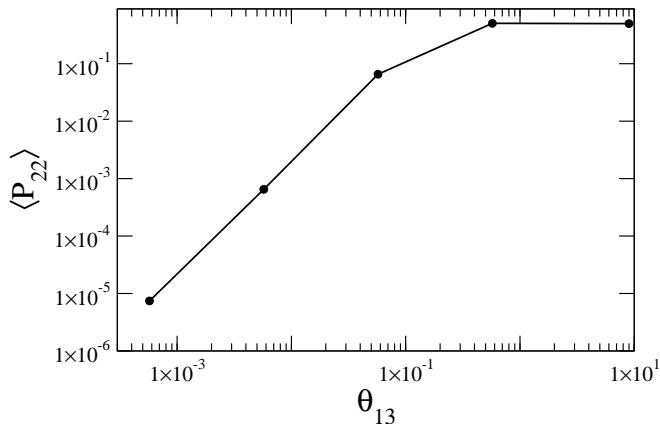


FIG. 9: Mean value of the second matter eigenstate for $E = 25$ MeV neutrinos as a function of third neutrino mixing angle, in degrees, for the case of normal hierarchy and $C_* = 0.1$.

0.02° or, equivalently, $\sin^2(2\theta_{13}) \gtrsim 4 \times 10^{-7}$.

B. Three flavor resonant and non-resonant mixing

To complete our study of turbulence effects we look at large amplitude fluctuations, their breaking of HL factorization and the impact in the channels where no MSW resonance(s) occur. We take the case of normal hierarchy as an example so the non-L-resonant and non-H-resonant transitions occur for antineutrinos. In figure (10) we present the turbulence density profile and the corresponding neutrino and anti-neutrino probabilities for the case of $\sin^2(2\theta_{13}) = 4 \times 10^{-4}$ and $C_*^2 = 0.34$. The amplitude of the fluctuations here is so large that HL factorization is broken. This can be seen from the evolution of P_{11} in the middle panel and noting that it occurs at the point where V_e in the top panel approaches the L resonance at $r \sim 60,000$ km. Also note that that breaking HL factorization does not depend upon the hierarchy. In the lower panel we see that simultaneously there is a sudden change in the anti-neutrino transition probabilities \bar{P}_{11} and \bar{P}_{12} at the point where the L resonance occurs but we do not observe any variation of \bar{P}_{13} which remains at zero for all r in this case. In order to observe non-trivial evolution of \bar{P}_{13} we need to increase θ_{13} close to the Chooz limit. An example with much larger θ_{13} is shown in figure (11) for the case of $\theta_{13} = 9^\circ$ and $C_*^2 = 0.1$. Again HL is broken, this time at $r \sim 50,000$ km, causing a sudden decrease in P_{11} and simultaneous jumps in \bar{P}_{11} and \bar{P}_{12} but we also notice from the lower panel that \bar{P}_{13} is already non-zero by this point; mixing between states $\bar{\nu}_1$ and $\bar{\nu}_3$ had commenced when V_e approached the H resonance at $r \sim 40,000$ km as shown in the top panel. Both these non resonant mixing effects can be understood through the antineutrino

non-adiabaticity parameters $\bar{\Gamma}_{12}$ and $\bar{\Gamma}_{13}$ which depend upon the derivatives of the matter mixing angles $\tilde{\theta}_{12}$ and $\tilde{\theta}_{13}$ respectively. For both, the matter mixing angle varies between the high density limit of zero to its value in vacuum at resonances. For $\tilde{\theta}_{12}$ this occurs at L resonances, for $\tilde{\theta}_{13}$ at H resonances. Thus we expect that the larger the value of the vacuum angle the greater the derivative and the non-adiabaticity parameters $\bar{\Gamma}_{12}$ and $\bar{\Gamma}_{13}$ and, therefore, the greater the mixing between the matter eigenstates $\bar{\nu}_1$ and $\bar{\nu}_2$ or $\bar{\nu}_1$ and $\bar{\nu}_3$. The difference between the mixing of neutrinos states $\bar{\nu}_1$ - $\bar{\nu}_2$ and $\bar{\nu}_1$ - $\bar{\nu}_3$ is that the vacuum value of θ_{12} is well known and large while the value of θ_{13} is neither large nor known. This effect of non-resonant mixing between states $\bar{\nu}_1$ and $\bar{\nu}_3$ is the same as found in Ref.[31] where it is also shown that the turbulence impact on the non-resonant neutrino channel disappears for a decreasing value of θ_{13} though we would like to emphasize that our findings are for a

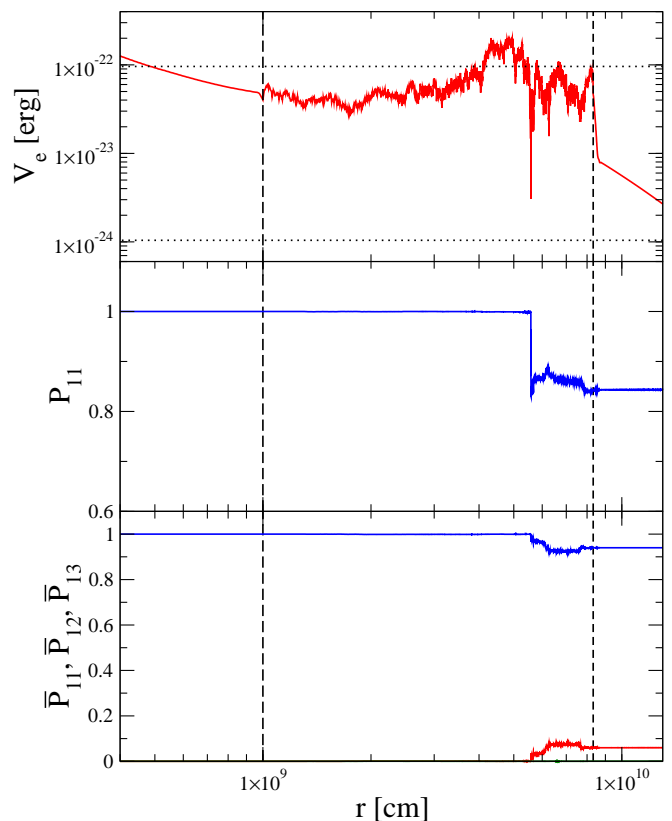


FIG. 10: Impact of turbulence on the first matter eigenstates for the neutrino survival probability (middle) and for the anti-neutrino survival and appearance probabilities (bottom). The results correspond to normal hierarchy, $\sin^2(2\theta_{13}) = 4 \times 10^{-4}$, $C_*^2 = 0.34$ and $E = 25$ MeV. The top panel shows the matter density profile with noise and again the vertical dashed lines indicate the turbulence region while the upper horizontal line is the H resonance and the lower the L resonance for this particular neutrino energy computed using the two-flavor formula.

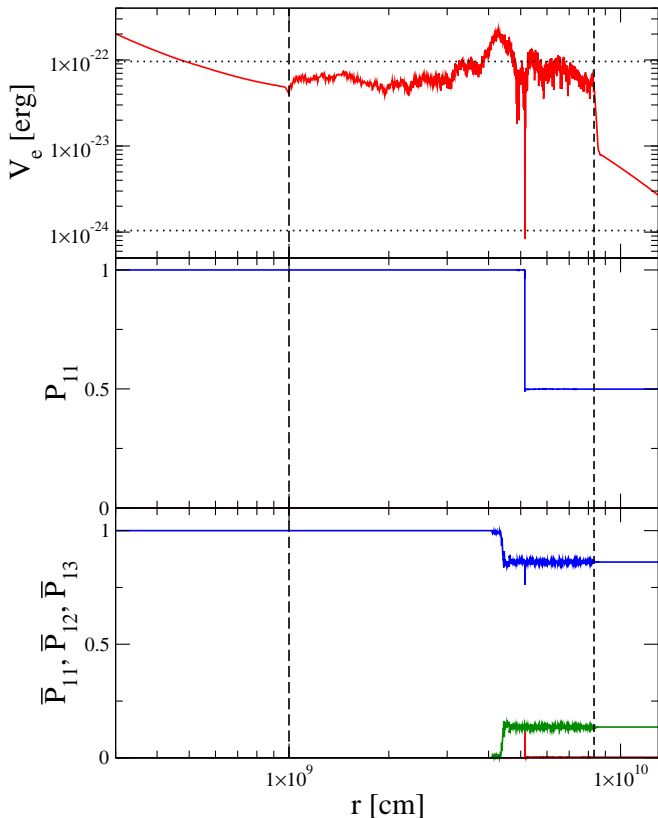


FIG. 11: Impact of turbulence on the first matter eigenstates for the neutrino survival probability (middle) and for the anti-neutrino survival and appearance probabilities (bottom). The results correspond to normal hierarchy, $\theta_{13} = 9^\circ$, $C_\star^2 = 0.1$ and $E = 25$ MeV. The top panel shows the matter density profile with noise and, like figure (10), the vertical dashed lines indicate the turbulence region while the upper horizontal line is the H resonance and the lower the L resonance for this particular neutrino energy computed using the two-flavor formula.

very different set-up than the one in [31]. It is important to note that the non-resonant effect from $\tilde{\theta}_{12}$ does not depend upon the hierarchy, it will always occur for the anti-neutrinos and never for the neutrinos because the sign of δm_{12}^2 is known. In contrast the non-resonant effect from $\tilde{\theta}_{13}$ will switch to the neutrinos if we consider an inverted hierarchy.

Thus we find two effects from turbulence in the non resonant channels. One from broken HL factorization causing non-L-resonant transitions and the other from the constant transitions from the high density to vacuum values of θ_{13} . As with the case of small θ_{13} and the H resonant channel, the distributions of the non resonant transition probabilities for an ensemble have an exponential like behavior. An example of the distributions for the particular case of for a normal hierarchy, $\theta_{13} = 9^\circ$, $C_\star^2 = 0.2$ and $E = 25$ MeV is shown in figure (12). As explained above, the average values of the distribu-

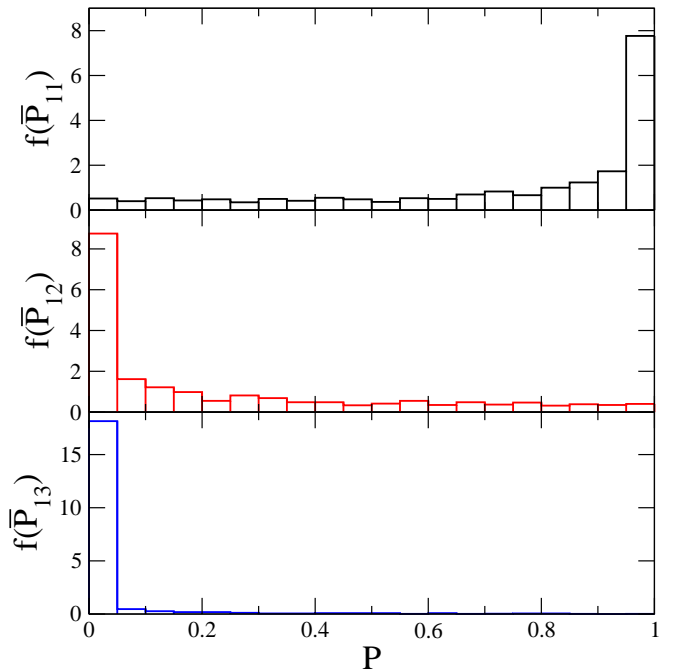


FIG. 12: Frequency distribution for the anti-neutrino probabilities for a normal hierarchy, $\theta_{13} = 9^\circ$, $C_\star^2 = 0.2$ and $E = 25$ MeV.

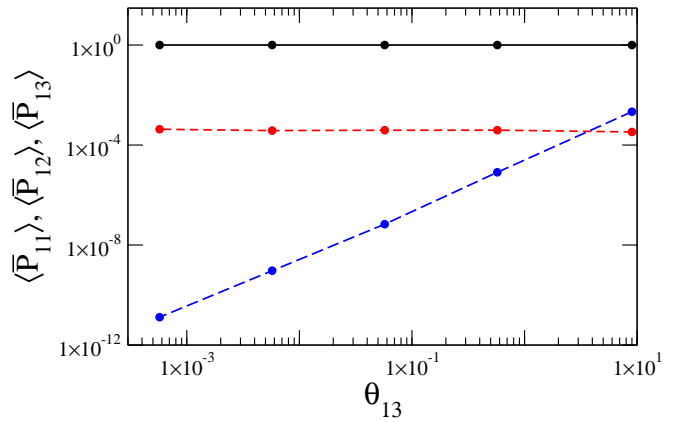


FIG. 13: Variation of the mean anti-neutrino survival probabilities $\langle \bar{P}_{11} \rangle$ (solid), $\langle \bar{P}_{12} \rangle$ (short dashed) and $\langle \bar{P}_{13} \rangle$ (long dashed) as a function of the vacuum mixing angle θ_{13} for the case of a normal hierarchy, $C_\star = 0.1$ and $E = 25$ MeV. The symbols indicate the values of θ_{13} where averages were calculated.

tions scale differently with θ_{13} and the variation of the turbulence effect with the third neutrino mixing angle is shown in figure (13). While the first matter eigenstate survival probability and appearance probability to the second matter eigenstate $\langle \bar{P}_{12} \rangle$ are constant the mixing with the third matter eigenstate, $\langle \bar{P}_{13} \rangle$, scales as θ_{13}^2 and so disappears as θ_{13} decreases. We also observe that the mixing between states $\bar{\nu}_1$ and $\bar{\nu}_3$ surpasses that between

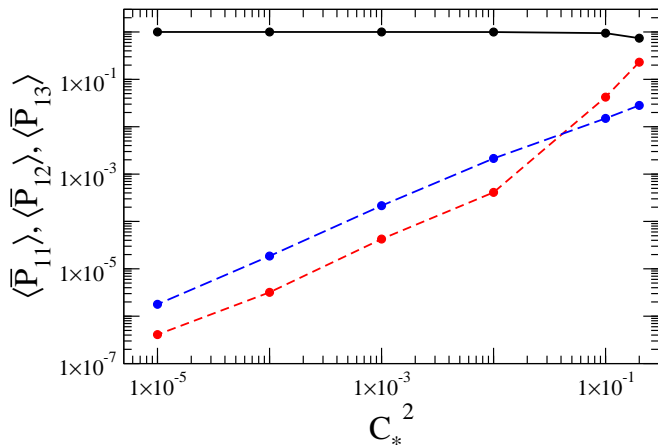


FIG. 14: Variation of the mean anti-neutrino survival probabilities $\langle \bar{P}_{11} \rangle$ (solid), $\langle \bar{P}_{12} \rangle$ (short dashed) and $\langle \bar{P}_{13} \rangle$ (long dashed) as a function of the fluctuation amplitude C_* for a vacuum mixing angle $\theta_{13} = 9^\circ$, the case of a normal hierarchy, and $E = 25$ MeV. The symbols indicate the values of C_* where averages were calculated.

$\bar{\nu}_1$ and $\bar{\nu}_2$ only for $\theta_{13} \geq 3^\circ$. Finally, the behavior of $\langle \bar{P}_{11} \rangle$, $\langle \bar{P}_{12} \rangle$ and $\langle \bar{P}_{13} \rangle$ as a function of the fluctuation amplitude C_*^2 is shown in Fig.(14). At small amplitudes both $\langle \bar{P}_{12} \rangle$ and $\langle \bar{P}_{13} \rangle$ scale as C_*^2 but as C_*^2 increases $\langle \bar{P}_{12} \rangle$ appears to increase its sensitivity to this parameter.

IV. CONCLUSIONS

We have performed a detailed investigation of turbulence effects after solving the evolution equation for neutrinos passing through turbulent density profiles created by adding matter density fluctuations to a 1D density profile obtained from hydrodynamical simulations. Our treatment differs from most previous studies since we do not solve the neutrino evolution equations for the averaged probabilities but rather for the neutrino amplitudes. The results have highlighted new turbulence effects for that period when the shocks are in the region of the H resonance for neutrino energies of order $\mathcal{O}(10$ MeV) and can be summarized as follows.

- For large third neutrino mixing angle but fluctuation amplitudes below $C_*^2 \sim 0.1$ we find turbulence effects only appear in the channel with the H resonance i.e. the neutrinos for a normal hierarchy, the antineutrinos for an inverted hierarchy. More specifically we find that if the matter density fluctuation amplitudes are tiny, no turbulence effects appear as expected; for intermediate values, $10^{-10} \lesssim C_*^2 \lesssim 10^{-2}$ the neutrino matter survival probabilities are dominated by the phase effects between the pre-existing resonances of the profile but with fluctuating relative phase that are sufficient to produce a wide variation of the final

states; for larger values of the matter density fluctuation amplitude, $10^{-2} \lesssim C_*^2 \lesssim 10^{-1}$, turbulence effects begin to dominate and lead to two-flavor depolarization. The sensitivity to amplitudes as small 0.001% would apparently indicate that turbulence effects in this channel are inevitable but, at the same time, observationally turbulence effects will be difficult to distinguish from phase effects once one takes into account time and energy binning of a signal, as pointed out in Galais *et al.* [21].

- When the matter density fluctuation amplitude is large, $C_*^2 \gtrsim 0.1$, we have found a sensitivity in the H resonant channel to the third neutrino mixing angle below the Dighe-Smirnov threshold down to $\sin^2(2\theta_{13}) \gtrsim 4 \times 10^{-7}$.
- Large amplitude matter density fluctuations, $C_*^2 \gtrsim 0.1$, lead to broken HL independent of θ_{13} and the hierarchy. This leads to resonant mixing between states ν_1 and ν_2 and non-resonant mixing between states $\bar{\nu}_1$ and $\bar{\nu}_2$.
- Once again, for large amplitude matter density fluctuations, $C_*^2 \gtrsim 0.1$, we find that non-resonant mixing may occur due to the fluctuations of the matter mixing angle $\tilde{\theta}_{13}$. The degree of mixing is a function of θ_{13} with a mean value that scales as θ_{13}^2 . The channel where this effect appears depends upon the hierarchy appearing in the antineutrinos for a normal hierarchy where it leads to mixing between $\bar{\nu}_1$ and $\bar{\nu}_3$ and in the neutrinos for an inverted hierarchy where it causes mixing between states ν_2 and ν_3 .

When the matter density fluctuations are small turbulence can only cause two flavor mixing. When the amplitude is large three flavor mixing may occur in the neutrinos and antineutrinos simultaneously but, depending upon the hierarchy and θ_{13} , not necessarily to the same degree. Let us summarize our findings in this case of large amplitude fluctuations:

- In the case of normal hierarchy: for θ_{13} above the Dighe-Smirnov threshold strong mixing occurs in the neutrinos and 3-flavor depolarization may be approached. On the other hand, if θ_{13} is close to the Chooz limit, 3-flavor mixing of the antineutrinos occurs, due to the two non-resonant effects; otherwise only two-flavor mixing takes place because of the non-resonant effect from $\tilde{\theta}_{12}$ fluctuations. When θ_{13} is below the Dighe-Smirnov threshold, the neutrinos still exhibit three flavor mixing due to broken HL factorization and the residual sensitivity to θ_{13} , that scales as θ_{13}^2 .
- In the case of inverted hierarchy: for large fluctuations and θ_{13} close to the Chooz limit, 3-flavor mixing occurs in the neutrinos, due to broken HL factorization, and the non-resonant effect from

$\tilde{\theta}_{13}$ fluctuations which will turn into 2-flavor non-resonant mixing of ν_1 and ν_2 as θ_{13} decreases. Three flavor mixing of the antineutrinos takes place for θ_{13} , above the Dighe-Smirnov threshold, but it is unlikely that depolarization is reached because the mixing between $\bar{\nu}_1$ and $\bar{\nu}_2$ is non-resonant. For θ_{13} below the Dighe-Smirnov threshold, some residual three-flavor mixing will remain, but it will be small, because now the two turbulence effects are perturbative in this channel.

Several aspects related to turbulence remain open. While our treatment of turbulence can already be considered, in many respects, realistic it is clear that future studies are awaited where matter density fluctuations are drawn from successful core-collapse supernova simulations at many different epochs. Also, until we can calibrate these one-dimensional studies the actual turbulence effects we should expect is unknown.

Lastly, one important question that needs further investigation is the extent of the ‘smearing’ or ‘blurring’ of turbulence features in a burst signal. Smearing can occur due several reasons. First there is the smearing due to the finite size of the source. The neutrinos we shall receive from the next Galactic supernova will not travel

along a single line of sight so the neutrino flux at a given arrival time and neutrino energy (ignoring time of flight issues [43]) is ‘averaged’ over a column of ~ 20 km i.e. the apparent diameter of the proto-neutron star source. Neutrinos emitted from different locations upon the source will pass through different small scale, $\lesssim 20$ km, fluctuations but the turbulence on large scales will be the same for all the neutrinos we receive in the burst. Second, a smearing in energy will occur in the detector due to the intrinsic energy resolution of the detection reaction and the extrinsic resolution of the detector. If the combined effect of intrinsic and extrinsic resolutions leads to a smearing over an energy range σ then features on scales smaller than σ will be unobservable. Finally, smearing in both time and energy will also be introduced because of the necessity of binning the detected events. As with the detector response, short time scale changes in the flux or features with small energy widths will be smeared reducing their observability. Studying how all these effects impact the observability of the turbulence effects pointed out in the present paper is not trivial and will be the object of future investigations. [41].

-
- [1] A. Mezzacappa, *Ann. Rev. Nucl. Part. Sci.* **55** 467 (2005).
[2] Blondin, J. M., Mezzacappa, A. and DeMarino, C., *Astrophys. J.* **584** 971 (2003)
[3] H. Duan, G. M. Fuller, J. Carlson and Y. Z. Qian, *Phys. Rev. D* **74** 105014 (2006) [arXiv:astro-ph/0606616].
[4] S. Hannestad, G. G. Raffelt, G. Sigl and Y. Y. Wong, *Phys. Rev. D* **74** 105010 (2006) [Erratum-ibid. *Phys. Rev. D* **76** 029901 (2007)] [arXiv:astro-ph/0608695].
[5] A. B. Balantekin and Y. Pehlivan, *J. Phys. G* **34** (2007) 47 [arXiv:astro-ph/0607527].
[6] G. G. Raffelt and A. Y. Smirnov, *Phys. Rev. D* **76** 125008 (2007) [arXiv:0709.4641 [hep-ph]].
[7] B. Dasgupta, A. Dighe, G. G. Raffelt and A. Y. Smirnov, *Phys. Rev. Lett.* **103** 051105 (2009) [arXiv:0904.3542 [hep-ph]].
[8] J. Gava and C. Volpe, *Phys. Rev. D* **78** 083007 (2008) [arXiv:0807.3418 [astro-ph]].
[9] R. C. Schirato and G. M. Fuller, arXiv:astro-ph/0205390.
[10] K. Takahashi, K. Sato, H. E. Dalhed and J. R. Wilson, *Astropart. Phys.* **20** 189 (2003) [arXiv:astro-ph/0212195].
[11] G. L. Fogli, E. Lisi, D. Montanino and A. Mirizzi, *Phys. Rev. D* **68** 033005 (2003) [arXiv:hep-ph/0304056].
[12] R. Tomas, M. Kachelriess, G. Raffelt, A. Dighe, H. T. Janka and L. Scheck, *JCAP* **0409** 015 (2004) [arXiv:astro-ph/0407132].
[13] G. L. Fogli, E. Lisi, A. Mirizzi and D. Montanino, *JCAP* **0504** 002 (2005) [arXiv:hep-ph/0412046].
[14] S. Choubey, N. P. Harries and G. G. Ross, *Phys. Rev. D* **74** 053010 (2006) [arXiv:hep-ph/0605255].
[15] J. P. Kneller and G. C. McLaughlin, *Phys. Rev. D* **73** 056003 (2006) [arXiv:hep-ph/0509356].
[16] B. Dasgupta and A. Dighe, *Phys. Rev. D* **75** 093002 (2007) [arXiv:hep-ph/0510219].
[17] H. Duan and J. P. Kneller, *J. Phys. G* **36** 113201 (2009) [arXiv:0904.0974 [astro-ph.HE]].
[18] H. Duan, G. M. Fuller and Y. Z. Qian, arXiv:1001.2799 [hep-ph].
[19] J. Gava, J. Kneller, C. Volpe and G. C. McLaughlin, *Phys. Rev. Lett.* **103** 071101 (2009) [arXiv:0902.0317 [hep-ph]].
[20] S. Chakraborty, S. Choubey, B. Dasgupta and K. Kar, *JCAP* **0809** 013 (2008) [arXiv:0805.3131 [hep-ph]].
[21] S. Galais, J. Kneller, C. Volpe and J. Gava, *Phys. Rev. D* **81** 053002 (2010) [arXiv:0906.5294 [hep-ph]].
[22] Kifonidis, K., Plewa, T., Scheck, L., Janka, H.-T., Müller, E., *Astron. Astrophys.* **453** 661 (2006)
[23] Scheck, L., Kifonidis, K., Janka, H.-T., Müller, E., *Astron. & Astroph.* **457** 963 (2006)
[24] Guzman, J., & Plewa, T., *Nonlinearity* **22** 2775 (2009)
[25] Sawyer, R. F., *Phys. Rev. D* **42** 3908 (1990) [Erratum-ibid. *Phys. Rev. D* **50** 1167 (1994)]
[26] Nunokawa, H., Rossi, A., Semikoz, V. B., & Valle, J. W. F., *Nuclear Physics B* **472** 495 (1996)
[27] Balantekin, A. B., Fetter, J. M., & Loreti, F. N., *Phys. Rev. D* **54** 3941 (1996)
[28] Hirota, K., *Phys. Rev. D* **57** 3140 (1998)
[29] F. N. Loreti and A. B. Balantekin, *Phys. Rev. D* **50** 4762 (1994) [arXiv:nucl-th/9406003].
[30] F. N. Loreti, Y.-Z. Qian, G. M. Fuller and A. B. Balantekin, nucleosynthesis”, *Phys. Rev. D* **52** 6664 (1995) [arXiv:astro-ph/9508106].
[31] G. Fogli, E. Lisi, A. Mirizzi and D. Montanino, *JCAP*

- 0606** 012 (2006) [arXiv:hep-ph/0603033]
- [32] A. Friedland and A. Gruzinov, arXiv:astro-ph/0607244.
- [33] J. P. Kneller, arXiv:1004.1288 [hep-ph].
- [34] C. Amsler et al. [Particle Data Group], Phys. Lett. B **667** 1 (2008).
- [35] Apollonio, M., & Baldini, A., Physics Letters B **466** 415 (1999)
- [36] Apollonio, M., et al., Physics Letters B **472** 434 (2000)
- [37] A. B. Balantekin, J. Gava and C. Volpe, Phys. Lett. B **662** 396 (2008) [arXiv:0710.3112 [astro-ph]].
- [38] J. P. Kneller, G. C. McLaughlin and J. Brockman, Phys. Rev. D **77** 045023 (2008) [arXiv:0705.3835 [astro-ph]].
- [39] A.J. Majda & P.R. Kramer, Phys. Rep. **314** 237 (1999).
- [40] Kneller, J. P., & McLaughlin, G. C., Phys. Rev. D **80** 053002 (2009)
- [41] J. Kneller and C. Volpe, in preparation.
- [42] A. S. Dighe and A. Yu. Smirnov, supernova”, Phys. Rev. D **62** 033007 (2000)
- [43] Beacom, J. F., & Vogel, P., Phys. Rev. D **58** 093012 (1998)